Virology **285,** 21–29 (2001)
doi:10.1006/viro.2001.0932, available online at http://www.idealibrary.com on IDEAL®

Mouse Hepatitis Virus Replicase Protein Complexes Are Translocated to Sites of M Protein Accumulation in the ERGIC at Late Times of Infection

Anne G. Bost, Erik Prentice, and Mark R. Denison[1]

Department of Microbiology and Immunology, Department of Pediatrics, and the Elizabeth B. Lamb Center for Pediatric Research, Vanderbilt University, Nashville, Tennessee 37232

Received July 28, 2000; returned to author for revision August 31, 2000; accepted March 25, 2001

The coronavirus mouse hepatitis virus (MHV) directs the synthesis of viral RNA on discrete membranous complexes that are distributed throughout the cell cytoplasm. These putative replication complexes are composed of intimately associated but biochemically distinct membrane populations, each of which contains proteins processed from the replicase (gene 1) polyprotein. Specifically, one membrane population contains the gene 1 proteins p65 and p1a-22, while the other contains the gene 1 proteins p28 and helicase, as well as the structural nucleocapsid (N) protein and newly synthesized viral RNA. In this study, immunofluorescence confocal microscopy was used to define the relationship of the membrane populations comprising the putative replication complexes at different times of infection in MHV-A59-infected delayed brain tumor cells. At 5.5 h postinfection (p.i.) the membranes containing N and helicase colocalized with the membranes containing p1a-22/p65 at foci distinct from sites of M accumulation. By 8 to 12 h p.i., however, the membranes containing helicase and N had a predominantly perinuclear distribution and colocalized with M. In contrast, the p1a-22/p65-containing membranes retained a peripheral, punctate distribution at all times of infection and did not colocalize with M. By late times of infection, helicase, N, and M each also colocalized with ERGIC p53, a specific marker for the endoplasmic reticulum–Golgi–intermediate compartment. These data demonstrated that the putative replication complexes separated into component membranes that relocalized during the course of infection. These results suggest that the membrane populations within the MHV replication complex serve distinct functions both in RNA synthesis and in delivery of replication products to sites of virus assembly.

INTRODUCTION

The coronavirus mouse hepatitis virus, strain A59 (MHV-A59), contains a 32-kb, single-stranded, positive-sense RNA genome. The MHV replicase gene (gene 1) encodes two coamino-terminal polyproteins that are proteolytically processed to yield at least 15 mature proteins (Fig. 1) (Denison *et al.,* 1998; Lu *et al.,* 1998; Ziebuhr and Siddell, 1999). Inhibition of gene 1 polyprotein processing at any time during infection has been shown to inhibit viral RNA synthesis (Kim *et al.,* 1995), demonstrating an essential role for proteolytically mature gene 1-encoded proteins in coronavirus replication and transcription. Studies of temperature-sensitive mutants of MHV have also implicated these proteins in viral RNA synthesis (Baric *et al.,* 1990; Leibowitz *et al.,* 1982; Schaad *et al.,* 1990). Yet, most of the MHV replicase gene products have no defined functions or sequence homology to known viral or cellular proteins.

Studies of the localization and interactions of MHV replicase proteins in infected cells have provided critical insights into the possible roles for these proteins during viral replication. The localization of replicase gene-encoded proteins to cytoplasmic foci active in viral RNA synthesis has been well documented (Bi *et al.,* 1995, 1998; Bost *et al.,* 2000; Denison *et al.,* 1999; Heusipp *et al.,* 1997; Schiller *et al.,* 1998; Shi *et al.,* 1999; van der Meer *et al.,* 1999; Ziebuhr and Siddell, 1999). In addition, recent confocal microscopy studies have determined that multiple replicase gene proteins are colocalized in these foci at 6.5 h postinfection (p.i.) (Bost *et al.,* 2000). Cell fractionation experiments have demonstrated association of the colocalized gene 1-encoded proteins with two membrane populations of distinct density on iodixanol gradients (Sims *et al.,* 2000). The less dense membrane population was LAMP-1 (lysosome-associated membrane protein 1) positive and contained the p65 and p1a-22 proteins (Sims *et al.,* 2000). In contrast, the more dense population contained markers for ER as well as LAMP-1-positive membranes. The dense population was associated with the viral helicase (hel), p28, and nucleocapsid (N) proteins (Sims *et al.,* 2000). In addition, the hel/p28/N-positive membranes contained almost all of the viral RNA synthesized between 6 and 8 h p.i. Finally, it has been shown that the putative replication com-

[1] To whom correspondence and reprint requests should be addressed at Department of Pediatrics, Vanderbilt University Medical Center, D7235 MCN, Nashville, TN 37232-2581. Fax: (615) 343-9723. E-mail: mark.denison@mcmail.vanderbilt.edu.

0042-6822/01 $35.00

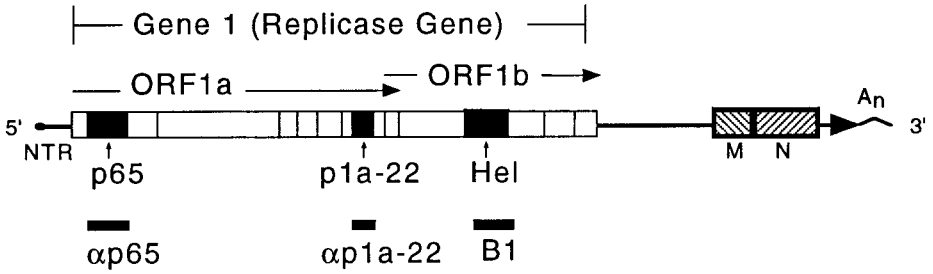

FIG. 1. MHV-A59 genome organization, replicase protein domains, and antibodies. The schematic of the 32-kb positive-strand RNA genome of MHV-A59 is shown. The overlapping open reading frames (ORFs 1a and 1b) are shown by arrows. The complete pattern of known and predicted mature proteins processed from the gene 1 replicase polyproteins is shown as domains demarcated by vertical lines. The regions of the genome expressing the M and N proteins are shown by hatched boxes. Mature replicase gene products discussed in this article are indicated by the black boxes. The black rectangles underneath the schematic represent regions of gene 1 expressed as recombinant proteins and used to generate polyclonal antisera (anti-p65, anti-p1a-22, and B1/αhel). NTR, nontranslated region; hel, helicase; M, membrane protein; N, nucleocapsid.

plexes were almost entirely discrete from sites of M accumulation (Bost *et al.,* 2000). Together, these data suggested that the putative MHV replication complex is multipartite, composed of closely associated membrane populations containing hel/N/p28/RNA and p1a-22/p65, respectively (Sims *et al.,* 2000), and that the multipartite complexes were distinct from sites of virion assembly. For simplicity in the current report, the term "complex" will be used to refer to colocalized proteins contained in the discrete membrane populations.

In this study we sought to determine whether the hel/N complexes remain associated with the p1a-22/p65 complexes throughout the infectious cycle in delayed brain tumor (DBT) cells. Experiments were performed to determine whether the localization of the hel/N complexes was altered with respect to the p1a-22/p65 complexes and sites of virion assembly during the course of infection. We demonstrate that the hel/N complexes were extensively colocalized with the p1a-22/p65 complexes at 5.5 h p.i., but by 8 h p.i. the hel/N complexes colocalized with M while the p1a-22/p65 complexes were still detected as peripheral foci entirely distinct from sites of M accumulation. The results of this study suggest that the multipartite nature of the putative MHV replication complex has an important biological implication; the ability to separate into two complexes and translocate one of these complexes to sites of virus budding at late times of infection.

RESULTS

The hel/N complex relocalizes to sites of M accumulation at late times of infection

Using hel as a marker for the hel/N/p28/RNA complexes and M as a marker for sites of virion assembly, we sought to determine whether the localization of hel/N complexes changed during the course of infection. DBT cells were mock-infected or infected with MHV-A59 for 5.5, 8, or 12 h and probed with antibodies directed against hel (B1) and M (J.1.3), followed by analysis using confocal immunofluorescence microscopy (Fig. 2). These times were chosen since we have previously shown that the rate of MHV RNA synthesis is maximal at 5 to 6 h p.i. in DBT cells and production of progeny virus is still active at 12 h p.i. (Kim *et al.,* 1995).

Neither hel, M, nor N was detected in mock-infected DBT cells (Fig. 2A). In MHV-infected cells, hel and M were distinct at 5.5 h p.i., with hel detected as punctate cytoplasmic foci and M as a typical perinuclear "cap." However, when cells were probed at 8 and 12 h p.i., hel and M were no longer distinct, but rather were extensively colocalized (Figs. 2B and 2C). The colocalization of hel and M was detected in a more prominent perinuclear pattern similar to that seen with M alone at 5.5 h p.i. Although the degree of hel/M colocalization varied from cell to cell in the infected monolayer at each time point, the number of cells with significant hel/M colocalization increased between 6 and 8 h p.i. (data not shown). Hel/M colocalization was predominant by 12 h p.i. We therefore chose 5.5 and 12 h p.i. as the early and late time points for subsequent experiments.

To determine whether hel was relocalizing independent of the complexes containing hel, N, and viral RNA, we investigated whether other components of the complex also relocalized at sites of M accumulation by 12 h p.i. Nucleocapsid protein was chosen since it has previously been shown to colocalize with hel by both confocal immunofluorescence and biochemical fractionation (Denison *et al.,* 1998; Sims *et al.,* 2000). When a direct comparison of N and hel localization was performed at 5.5 h p.i., hel and N colocalized in punctate cytoplasmic foci (Fig. 2C), in agreement with our previous results (Denison *et al.,* 1998). When cells were probed for hel and N at 12 h p.i., hel and N retained their colocalization both in single cells and in syncytia (Fig. 2C). This result suggested that both hel and N were relocalizing in intact complexes at late times of infection. To demonstrate this directly, the localization of N with respect to M was

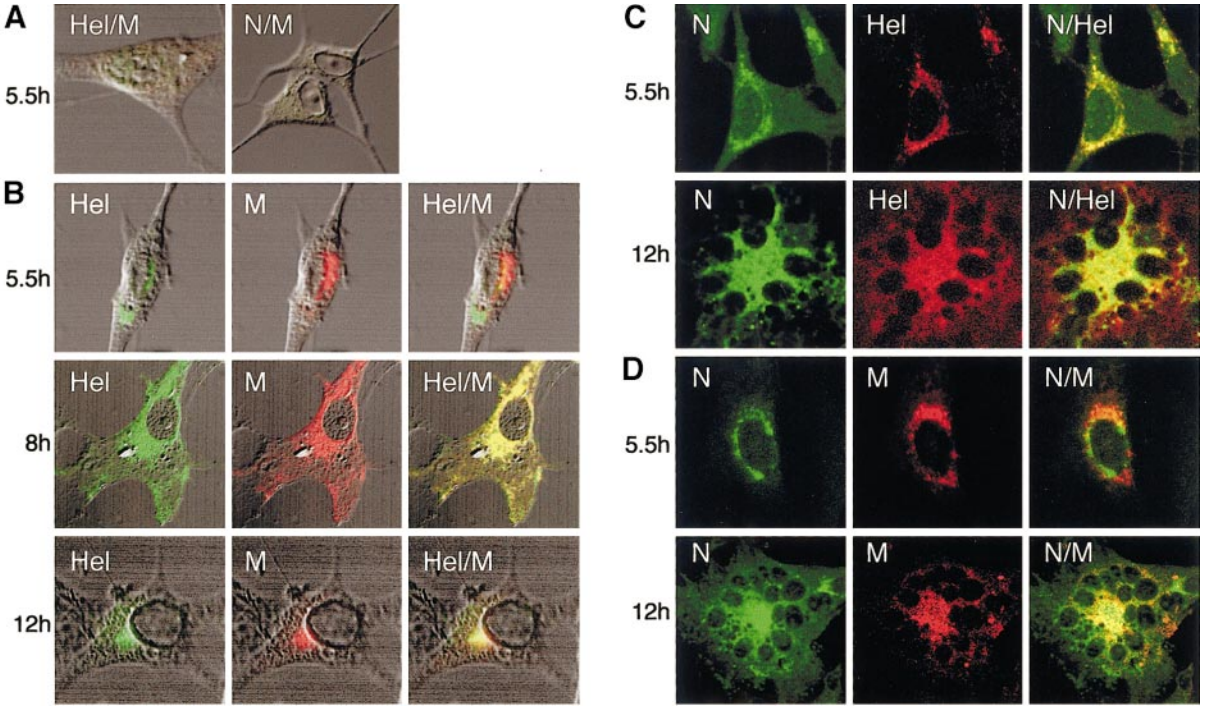

FIG. 2. Relocalization of hel/N complexes in MHV-infected DBT cells. MHV-A59-infected DBT cells were fixed and permeabilized at the times indicated (5.5, 8, or 12 h p.i.) and dual labeled. Yellow pixels in merged images indicate areas of coincidence of red and green signal. (A) Mock-infected DBT cells probed for hel (green) and M (red) (hel/M) or N (green) and M (red) (N/M). Red, green, and DIC images are merged to show cell morphology. (B) Localization of hel (green) and M (red) at 5.5, 8, and 12 h p.i. Images include DIC image to show morphology and lack of nuclear localization. (C) Colocalization of N (green) and hel (red) at 5.5 and 12 h p.i. Yellow pixels in right panels show coincidence of signal (D). Colocalization of N (green) and M (red) at 5.5 and 12 h p.i.

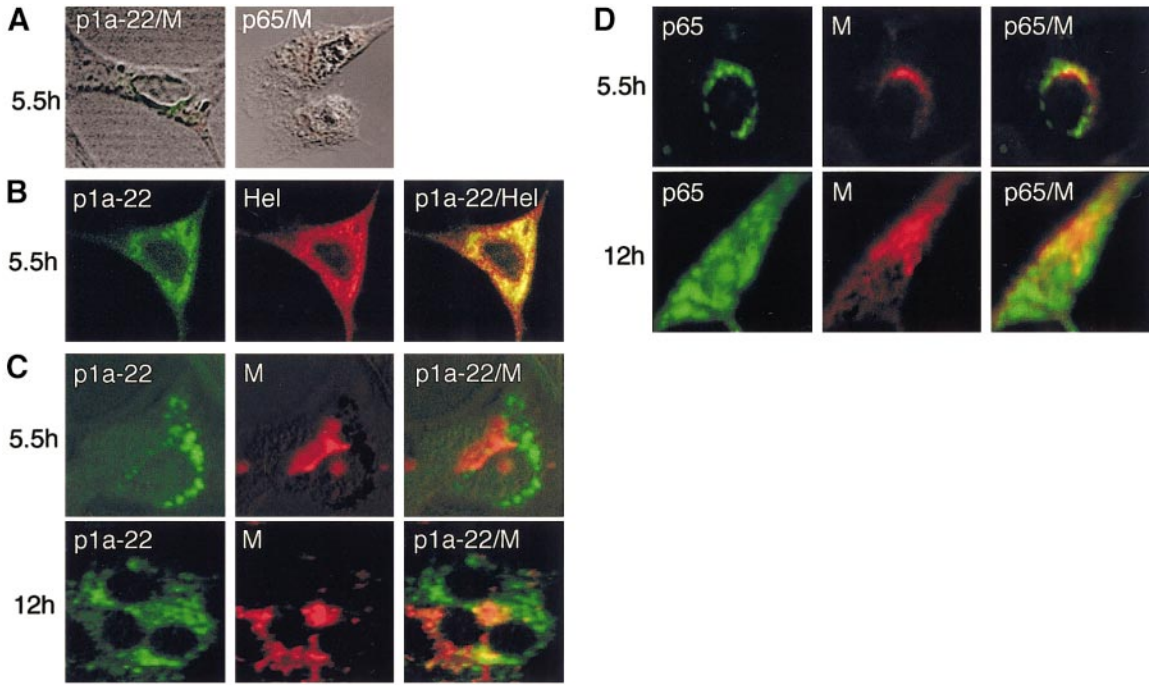

FIG. 3. p1a-22 and p65 do not relocalize during MHV infection. MHV-A59-infected DBT cells were fixed and permeabilized at 5.5 or 12 h and probed for M (red in all panels) and for either p1a-22 or p65 (green). Yellow pixels in merged images indicate areas of coincidence of red and green signal. (A) Mock-infected DBT cells probed for p1a-22 and M (p1a-22/M) or p65 and M (p65/M). Images are merged red, green, and DIC images. (B) Localization of p1a-22 (green) and hel (red) at 5.5 h p.i. (C) Localization of p1a-22 and M at 5.5 and 12 h p.i. (D) Localization of p65 and M at 5.5 and 12 h p.i.

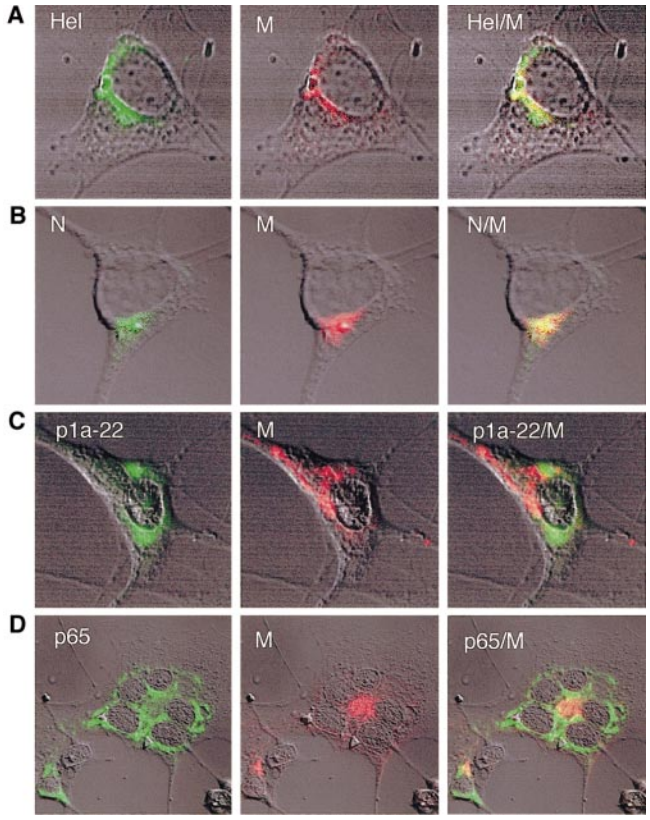

FIG. 4. Cycloheximide does not inhibit hel/N complex relocalization. MHV A59-infected DBT cells were treated with cycloheximide beginning at 5.5 h p.i. continuously until 12 h p.i., when cells were fixed and permeabilized. Cells were then probed for (A) hel and M; (B) N and M; (C) p1a-22 and M; or (D) p65 and M. M is red in all panels. Yellow pixels in merged images indicate areas of coincidence of red and green signal.

analyzed at 5.5 and 12 h p.i. At 5.5 h p.i., foci of N were entirely distinct from sites of M concentration, but by 12 h p.i., N was extensively colocalized with M in perinuclear foci, in a pattern indistinguishable from that with hel and M. The N/M colocalization was observed both in individual cells (data not shown) and in syncytia. Together these results demonstrated that the intact membranous complexes containing hel and N were relocalized to sites of M accumulation.

The hel/N complexes and p1a-22/p65 complexes separate at late times of infection

We next sought to determine whether the hel/N complexes remained associated with the p1a-22/p65 complexes throughout infection. MHV-infected cells were fixed at 5.5 and 12 h p.i. and localization of p1a-22 and p65 with respect to M was determined in dual-labeling experiments (Fig. 3). In mock-infected cells, no signal was detected with αp1a-22 or αp65, confirming the specificity of the antibodies (Fig. 3A). In MHV-infected cells, we first demonstrated that p1a-22 and hel colocalized extensively at 5.5 h p.i., a result consistent with our previous studies (Fig. 3B) (Bost *et al.,* 2000). When p1a-22 and M were directly compared at 5.5 h p.i., p1a-22 was detected in characteristic punctate cytoplasmic complexes that were completely distinct from the signal for M, typically found in a focused perinuclear pattern (Fig. 3C). At 12 h p.i., the pattern of p1a-22 with respect to M was unchanged, remaining completely distinct, and in dramatic contrast to the colocalization of hel and N with M at 12 h p.i. The observed separation of p1a-22 from M was not dependent on cell morphology and was not affected by syncytia formation.

When cells were probed for p65 and M, p65 was detected in a pattern identical to that of p1a-22, with punctate cytoplasmic foci of p65 in a pattern that was distinct from the perinuclear foci of M at all times of infection (Fig. 3D). These data confirmed that the p1a-22/p65-associated membranes were physically distinct from the hel/N-associated membranes and showed that the hel/N complexes and the p1a-22/p65 complexes separate during the course of infection.

Relocalization of hel/N complexes to sites of M accumulation does not require new protein synthesis

To demonstrate that the colocalization of hel/N complexes with M at late times postinfection was due to translocation of existing hel/N complexes to sites of M accumulation rather than to *de novo* synthesis of hel or N

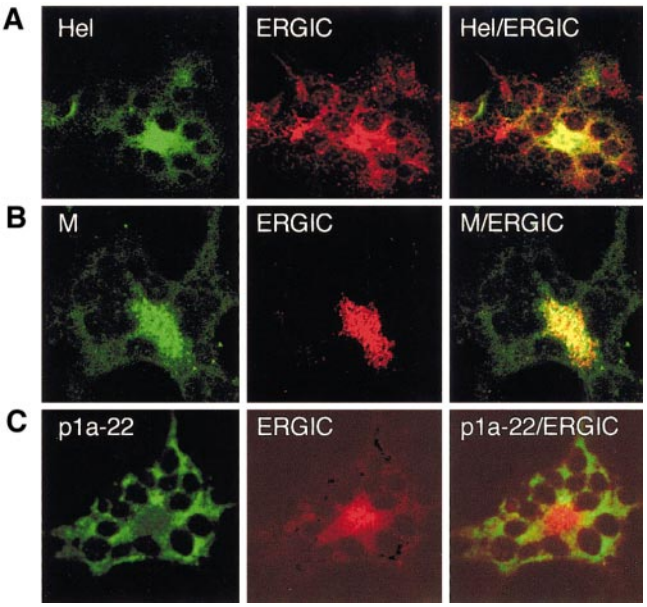

FIG. 5. Hel and M colocalize with ERGIC-p53 at late times of infection. MHV-infected cells were fixed and permeabilized at 12 h p.i. and probed for ERGIC-p53 (red in all panels) and hel, M, or p1a-22 (green). Merged images are shown to the far right with yellow pixels showing colocalization of red and green signal. (A) hel/ERGIC; (B) M/ERGIC; (C) p1a-22/ERGIC.

at a new location, we analyzed the effect of the translation inhibitor cycloheximide on hel/N relocalization (Fig. 4). A 100 μg/ml concentration of cycloheximide has been previously determined to be sufficient for inhibition of gene 1 translation in coronavirus-infected cells (Kim *et al.,* 1995; Perlman *et al.,* 1987; Sawicki and Sawicki, 1986). When infected cells were incubated with cycloheximide beginning at 5.5 h p.i. and continuing throughout the remainder of infection, extensive colocalization of hel or N with M was still observed at 12 h p.i. (Figs. 4A and 4B). In contrast, p1a-22 and p65 remained distinct from M at 12 h p.i. in the presence of cycloheximide (Figs. 4C and 4D). These experiments demonstrated that the observed colocalization of the hel/N complexes from 8 to 12 h p.i. was due to translocation of membrane-associated proteins translated prior to 5.5 h p.i. This experiment also showed that the process of translocation did not require ongoing cellular or viral protein synthesis between 5.5 and 12 h p.i.

Hel and M colocalize on endoplasmic reticulum–Golgi–intermediate compartment membranes at late times of infection

Coronavirus budding is known to take place in the endoplasmic reticulum–Golgi–intermediate compartment (ERGIC) (Klumperman *et al.,* 1994; Krijnse-Locker *et al.,* 1994). We therefore wanted to know whether the ERGIC was the site of colocalization of M with the hel/N complex. We used an antibody directed against ERGIC-p53, a specific marker for the ERGIC (Hauri *et al.,* 2000), to determine whether the ERGIC was the site of colocalization of hel/N complexes with M. DBT cells were infected for 5.5 h before the medium was changed to DMEM containing cycloheximide. Infected cells were fixed at 12 h p.i. and probed for ERGIC-p53 and either hel or M (Figs. 5A and 5B). At 12 h p.i. both hel and M colocalized with ERGIC-p53. In contrast, when cells were dual-labeled for p1a-22 and ERGIC-p53, p1a-22 was entirely distinct from ERGIC-p53 (Fig. 5C). These results showed that the hel/N complexes, but not the p1a-22/p65 complexes, were translocated to the MHV budding compartment in the ERGIC.

DISCUSSION

Positive-strand RNA viruses are known to organize replication complexes on the surface of cytoplasmic membranes using a variety of mechanisms and cytoplasmic organelles to organize their replication complexes (Candurra *et al.,* 1999; Froshauer *et al.,* 1988; Nejmeddine *et al.,* 2000; Schlegel *et al.,* 1996; Westaway *et al.,* 1997). However, several important areas of the cell biology of replication complex formation and function of positive-strand RNA viruses have remained undefined. One area critical to understanding virus–host interaction during replication is the changes that occur in viral replication complexes over time. This is important since biochemical and physical changes in the replication complexes may correlate with different stages of RNA transcription, replication, encapsidation, or assembly. The second question concerns the relationship of replication complexes to sites of virus assembly in cells. This is a particularly intriguing area since several positive-strand RNA viruses, such as the alphaviruses and flaviviruses, target replication complexes to sites that are distinct from those of virus assembly, raising questions about how newly synthesized RNA is delivered to these sites of assembly. Therefore, understanding the dynamic virus–host interactions is critical to a comprehensive understanding of replication.

In this study we have shown that there are temporal changes in the organization, association, and localization of the membrane/protein/RNA complexes that together comprise the putative mouse hepatitis virus replication complexes. Our previous confocal and biochemical experiments strongly argued that the membrane/protein complexes active in MHV RNA synthesis were in fact composed of two independent membrane populations containing distinct replicase (gene 1) proteins (Bost *et al.,* 2000; Sims *et al.,* 2000). The experiments in this study have demonstrated the physical separation of the hel/N and p1a-22/p65 complexes and relocalization of the hel/N complex during the course of infection, thus confirming in a compelling fashion that the MHV replication complexes are composed of physically distinct but closely associated membrane/protein populations. To our knowledge this is the first description of a multipartite replication complex with distinct temporal patterns of association and separation. The results have important implications for our study and understanding of the regulation of coronavirus RNA synthesis and virion assembly.

Localization of the hel/N complex and viral RNA

Our results show that the localization of both hel and N changes during the course of infection, characterized by decreasing interaction with the p1a-22/p65 complex and increasing colocalization with a marker for virion assembly, the structural protein M. Since we previously demonstrated that hel, N, p28, and newly synthesized viral RNA segregate to the same membrane population (Sims *et al.,* 2000), our present study strongly suggests that viral RNA and the p28 protein are also delivered with hel and N to the ERGIC. We have detected MHV RNA metabolically labeled with BrUTP at sites entirely distinct from the p1a-22/p65 complex at 6 to 8 h p.i. (data not shown); however, it has been more difficult to directly show the translocation of newly synthesized genomic RNA. We presume this is because it would require shut-

off of all viral RNA synthesis at 5–6 h p.i., tracking of RNA synthesized before inhibition of RNA synthesis, and stability of RNA over a 3- to 6-h period. Further, it has been reported that viral nucleocapsids are rapidly incorporated into virions and exported from the cell, so that localizing amounts of RNA necessary for detection at late times may be difficult. We are currently using a combination of metabolic labeling, RNA fluorescence *in situ* hybridization, and immuno-EM approaches to investigate the specific association of genomic RNA with the hel/N complex, as well as the predicted translocation of viral nucleocapsids for assembly over time.

Continued protein expression is not required for separation and translocation of the hel/N complex

Relocalization of the hel/N complexes occurred in the presence of inhibitory concentrations of cycloheximide, demonstrating that continued viral or cellular protein synthesis after 5.5 h p.i. was not required for separation or translocation of the complexes. Since addition of cycloheximide has been shown to result in the rapid shutoff of viral RNA synthesis when added at any time during infection (Kim *et al.,* 1995; Perlman *et al.,* 1987; Sawicki and Sawicki, 1986; Shi *et al.,* 1999), our experiments further suggest that continued RNA synthesis after 5.5 h may not be required for hel/N complex translocation. The separation and translocation observed may therefore be the result of viral or cellular processes or signals that are already under way prior to inhibition of viral protein or RNA synthesis. This is a reasonable possibility since MHV RNA synthesis also begins to decline by 6–8 h p.i. in untreated cells (Kim *et al.,* 1995). It should be possible to answer this question by investigating inhibition of viral or cellular protein or RNA synthesis at earlier times in infection.

Mechanisms of translocation of hel/N complexes

Another question that has arisen from our experiments is the mechanism of translocation of the hel/N complexes. We have previously reported that the membranes with which hel, N, RNA, and p28 segregate contain enzymatic activity found in membranes of the endoplasmic reticulum (ER) (NADPH–cytochrome C reductase) (Sims *et al.,* 2000). If the ER is the sole or major membrane component of hel/N complexes, then "normal" ER-to-ERGIC trafficking pathways would provide an established mechanism that MHV might exploit to deliver replication products to sites of assembly. It is interesting that the presence of distributed punctate ERGIC or "ER exit sites" has been recently described (Rossanese *et al.,* 1999) and that the pattern of expression of these sites is reminiscent of the MHV replication complexes at 5 to 6 h p.i. (Bost *et al.,* 2000; Shi *et al.,* 1999; van der Meer *et al.,* 1999). ER-to-ERGIC movement appears to be an ongoing process of migration of ER "packets" along microtubular highways in normal cells except in the presence of specific inhibitors (Thyberg and Moskalewski, 1999). Thus the temporal change in hel/N complex association with the p1a-22/p65 complex and the rather specific transition to separation and translocation suggest a regulated process. Since new virus is detected in the supernatant medium of MHV-infected DBT cells before the change in hel/N complex localization is observed, it is likely that translocation of smaller packets of hel/N complexes is occurring earlier than 6 h p.i. The prominent alteration in hel/N complex localization detected in this study may represent a more comprehensive transition from replication to assembly.

It is also possible that endosome-to-ERGIC trafficking could account for some or all hel/N complex translocation, since late endosomes have been implicated as sites for viral RNA synthesis (van der Meer *et al.,* 1999), and markers for endosomes have been detected in gradient fractions containing the hel/N/p28/RNA complexes (Sims *et al.,* 2000). There is no precedent for direct trafficking from endosomes to ERGIC; rather it is thought that endosome-to-ER trafficking occurs via retrograde movement through the Golgi. Specifically, Rab 9-mediated movement from endosomes to the *trans*-Golgi network (TGN) results in fusion of endosomes with the TGN (Lombardi *et al.,* 1993). The endosome cargo is then available for movement by retrograde transport mechanisms from the TGN to the ERGIC (White *et al.,* 1999). Identification of the membranes in the hel/N complex will be useful as a basis for investigating specific pathways of cellular transport.

Implications of hel/N complex translocation for virion assembly

Delivery of the hel/N complexes to sites of virus assembly also might serve an important function in assembly. In addition to serving as a potential mechanism for delivery of newly synthesized RNA, hel/N migration could serve as a retention signal for M in the ERGIC. Narayanan *et al.* (2000) have recently reported specific M–N interactions at 8 h p.i. in a pre-Golgi compartment; however, they were unable to re-create this interaction in cells overexpressing M and N. They speculated that a MHV-specific action is required for this interaction (Narayanan *et al.,* 2000). Our experiments would support the conclusion that the missing MHV action is the translocation of the hel/N complex. Additionally, it was reported that N was associated with all genomic and subgenomic RNA species, but only N in association with genome length RNA was able to be coimmunoprecipitated with M (Narayanan

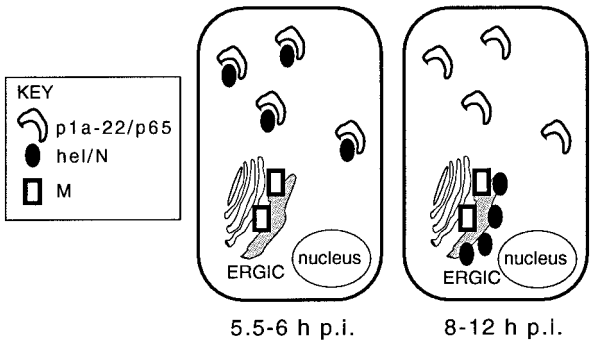

FIG. 6. Model of coronavirus replication complex separation and translocation of hel/N complexes to ERGIC. See text for discussion.

et al., 2000). Thus hel/N complex translocation provides an attractive model for regulation of packaging of complete viral nucleocapsids.

Model of coronavirus replication complex shuttling to sites of virion assembly

The events between coronavirus entry and assembly appear to involve a dynamic process of changing protein/membrane interactions. Based on our data, we propose a model in which virus–cell interactions may be divided into temporally distinct stages (Fig. 6). The early stage (0 to 6 h p.i.) is characterized by gene 1 replicase protein expression, maturation, and targeting to biochemically separate but intimately associated membrane populations in discrete foci within the cell cytoplasm. These interacting membrane populations are sites for viral RNA synthesis, with the timing of maximal detection of the interacting membrane/protein complexes corresponding to times of maximal viral RNA synthesis. During this stage, newly synthesized viral RNA associates specifically with the membrane population containing hel, N, and p28 (Bost *et al.,* 2000; Denison *et al.,* 1998; Kim *et al.,* 1995; Shi *et al.,* 1999; van der Meer *et al.,* 1999). Finally, during the early stage, M protein can be detected in perinuclear and cytoplasmic foci discrete from the putative replication complexes. During the intermediate stage (6 to 8 h p.i.), the translocation of hel/N complexes to the ERGIC is first observed. The late stage (8 to 12 h p.i.) is characterized by extensive separation of the hel/N complexes from the p1a-22/p65 complexes and colocalization of hel/N complexes with the ERGIC and M. This late stage is temporally associated with decreasing rates of new viral RNA synthesis and maximal rates of new virus production. We speculate that these temporal associations are not coincidental but rather reflect specific transitions in the virus life cycle from replication to assembly. This would further indicate that the association of p1a-22/p65 complexes with hel/N complexes is required for RNA synthesis and that the separation and translocation of the hel/N complexes result in both shutoff of RNA synthesis and delivery of viral nucleocapsids to sites of virion budding.

The results of this study will provide the foundation for studies of the mechanisms of replication complex formation, function, and translocation. The link between stages of replication and detectable virus cell interactions should allow us to define viral and cellular proteins and pathways involved in each stage of MHV replication.

MATERIALS AND METHODS

Antibodies

The anti-hel (B1), anti-p1a-22, and anti-p65 antisera were generated in rabbits and have been previously published (Denison *et al.,* 1999; Lu *et al.,* 1998; Sims *et al.,* 2000). The anti-M (J.1.3) and anti-N (J.3.3) monoclonals were provided by John Fleming (University of Wisconsin, Madison), and anti-ERGIC was obtained from Hans-Peter Hauri (University of Basel, Switzerland).

Virus infection and confocal immunofluorescence assays.

DBT cells on glass coverslips were mock-infected or infected with MHV A59 (Hirano *et al.,* 1976) at a multiplicity of infection of 10 plaque-forming units per cell. Infections were performed at 37°C in Dulbecco's modified Eagle's medium (DMEM) containing 6% fetal calf serum (FCS). In all experiments using cycloheximide, the virus inoculant was removed from the cells at 5.5 h p.i. and replaced with DMEM containing 6% FCS and 100 μg/ml cycloheximide (Sigma). DMEM in parallel mock-infected wells was also replaced with cycloheximide-containing medium at 5.5 h p.i. At the times indicated, cells were washed in 1× Tris and fixed in −20°C 100% methanol. Cells were then rehydrated in phosphate-buffered saline (PBS) containing 5% bovine serum albumin (BSA). For dual-labeling studies using one primary antibody derived from rabbit and the other from mouse, primary antisera were combined in diluent containing PBS with 2% goat serum, 1% BSA, and 0.05% NP-40 and were incubated with the rehydrated cells for 1 h at room temperature. Primary polyclonal sera were all used at a final 1:100 dilution for each antibody, and the monoclonal anti-N (J.3.3), anti-M (J.1.3), and anti-ERGIC antibodies were each diluted 1:500. After being washed in PBS/1% BSA/0.05% NP-40, cells were incubated at room temperature for 1 h with a 1:1000 dilution of anti-rabbit and/or anti-mouse secondary antisera conjugated to Alexa 488 or Alexa 546 dyes (Molecular Probes). The final antibody incubation for all cells was followed by washing in

PBS/1% BSA/0.05% NP-40. Cells were then washed with PBS, rinsed with H_2O, and mounted in Aquapolymount (Polysciences, Inc.) on glass slides. Immunofluorescence was detected at 488 and 543 nm using a 40× oil immersion objective on the Zeiss LSM 410 confocal microscope in the Shared Imaging Resource of the Vanderbilt Ingram Cancer Center. Differential interference contrast (DIC) images were obtained using the 488-nm laser. For images shown in color, red and green were artificially assigned to the grayscale images using the hue-saturation option in Adobe Photoshop 5.0.

ACKNOWLEDGMENTS

This work was supported by National Institutes of Health Grants AI-26603 and AI01479. We thank Hans-Peter Hauri at the University of Basel, Switzerland, for supplying anti-ERGIC, and John Fleming at the University of Wisconsin, for the J.1.3 and J.3.3 antibodies. In addition, we gratefully acknowledge the assistance of Jonathan Sheehan in the Molecular Imaging Shared Resource of the Vanderbilt Ingram Cancer Center (IP30CA68485). Finally, we are indebted to Amy Sims for critically reading the manuscript and to XiaoTao Lu for generation of the B1, anti-p1a-22, and anti-p65 antibodies.

REFERENCES

Baric, R. S., Fu, K., Schaad, M. C., and Stohlman, S. A. (1990). Establishing a genetic recombination map for murine coronavirus strain A59 complementation groups. *Virology* **177,** 646–656.

Bi, W., Bonilla, P. J., Holmes, K. V., Weiss, S. R., and Leibowitz, J. L. (1995). Intracellular localization of polypeptides encoded in mouse hepatitis virus open reading frame 1A. *Adv. Exp. Med. Biol.* **380**(251), 251–258.

Bi, W., Pinon, J. D., Hughes, S., Bonilla, P. J., Holmes, K. V., Weiss, S. R., and Leibowitz, J. L. (1998). Localization of mouse hepatitis virus open reading frame 1a derived proteins. *J. Neurovirol.* **4**(6), 594–605.

Bost, A. G., Carnahan, R. H., Lu, X. T., and Denison, M. R. (2000). Four proteins processed from the replicase gene polyprotein of mouse hepatitis virus colocalize in the cell periphery and adjacent to sites of virion assembly. *J. Virol.* **74**(7), 3399–3403.

Candurra, N., Lago, M., Maskin, L., and Damonte, E. (1999). Involvement of the cytoskeleton in Junin virus multiplication. *J. Gen. Virol.* **80,** 147–156.

Denison, M. R., Sims, A. C., Gibson, C. A., and Lu, X. T. (1998). Processing of the MHV-A59 gene 1 polyprotein by the 3C-like proteinase. *Adv. Exp. Med. Biol.* **440,** 121–127.

Denison, M. R., Spaan, W. J., van der Meer, Y., Gibson, C. A., Sims, A. C., Prentice, E., and Lu, X. T. (1999). The putative helicase of the coronavirus mouse hepatitis virus is processed from the replicase gene polyprotein and localizes in complexes that are active in viral RNA synthesis. *J. Virol.* **73**(8), 6862–6871.

Froshauer, S., Kartenbeck, J., and Helenius, A. (1988). Alphavirus RNA replicase is located on the cytoplasmic surface of endosomes and lysosomes. *J. Cell Biol.* **107**(6), 2075–2086.

Hauri, H., Kappeler, F., Andersson, H., and Appenzeller, C. (2000). ERGIC-53 and traffic in the secretory pathway. *J. Cell Sci.* **113,** 587–596.

Heusipp, G., Grotzinger, C., Herold, J., Siddell, S. G., and Ziebuhr, J. (1997). Identification and subcellular localization of a 41 kDa, polyprotein 1ab processing product in human coronavirus 229E-infected cells. *J. Gen. Virol.* **78**(Pt. 11), 2789–2794.

Hirano, N., Fujiwara, K., and Matumoto, M. (1976). Mouse hepatitis virus (MHV-2): Plaque assay and propagation in mouse cell line DBT cells. *Jpn. J. Microbiol.* **20**(3), 219–225.

Kim, J. C., Spence, R. A., Currier, P. F., Lu, X. T., and Denison, M. R. (1995). Coronavirus protein processing and RNA synthesis is inhibited by the cysteine proteinase inhibitor e64dd. *Virology* **208,** 1–8.

Klumperman, J., Locker, J. K., Meijer, A., Horzinek, M. C., Geuze, H. J., and Rottier, P. J. (1994). Coronavirus M proteins accumulate in the Golgi complex beyond the site of virion budding. *J. Virol.* **68**(10), 6523–6534.

Krijnse-Locker, J., Ericsson, M., Rottier, P. J., and Griffiths, G. (1994). Characterization of the budding compartment of mouse hepatitis virus: Evidence that transport from the RER to the Golgi complex requires only one vesicular transport step. *J. Cell Biol.* **124**(1–2), 55–70.

Leibowitz, J. L., DeVries, R. R., and Haspel, M. V. (1982). Genetic analysis of murine hepatitis virus strain JHM. *J. Virol.* **42,** 1080–1087.

Lombardi, D., Soldati, T., Riederer, M. A., Goda, Y., Zerial, M., and Pfeffer, S. R. (1993). Rab9 functions in transport between late endosomes and the trans Golgi network. *EMBO J.* **12**(2), 677–682.

Lu, X. T., Sims, A. C., and Denison, M. R. (1998). Mouse hepatitis virus 3C-like protease cleaves a 22-kilodalton protein from the open reading frame 1a polyprotein in virus-infected cells and in vitro. *J. Virol.* **72**(3), 2265–2271.

Narayanan, K., Maeda, A., Maeda, J., and Makino, S. (2000). Characterization of the coronavirus M protein and nucleocapsid interaction in infected cells. *J. Virol.* **74**(17), 8127–8134.

Nejmeddine, M., Trugnan, G., Sapin, C., Kohli, E., Svensson, L., Lopez, S., and Cohen, J. (2000). Rotavirus spike protein VP4 is present at the plasma membrane and is associated with microtubules in infected cells. *J. Virol.* **74**(7), 3313–3320.

Perlman, S., Reese, D., Bolger, E., Chang, L. J., and Stoltzfus, C. M. (1987). MHV nucleocapsid synthesis in the presence of cycloheximide and accumulation of negative strand MHV RNA. *Virus Res.* **6,** 261–272.

Rossanese, O. W., Soderholm, J., Bevis, B. J., Sears, I. B., O'Connor, J., Williamson, E. K., and Glick, B. S. (1999). Golgi structure correlates with transitional endoplasmic reticulum organization in *Pichia pastoris* and *Saccharomyces cerevisiae*. *J. Cell Biol.* **145**(1), 69–81.

Sawicki, S. G., and Sawicki, D. L. (1986). Coronavirus minus-strand RNA synthesis and effect of cycloheximide on coronavirus RNA synthesis. *J. Virol.* **57**(1), 328–334.

Schaad, M. C., Stohlman, S. A., Egbert, J., Lum, K., Fu, K., Wei, T. J., and Baric, R. S. (1990). Genetics of mouse hepatitis virus transcription: Identification of cistrons which may function in positive and negative strand RNA synthesis. *Virology* **177,** 634–645.

Schiller, J. J., Kanjanahaluethai, A., and Baker, S. C. (1998). Processing of the coronavirus MHV-JHM polymerase polyprotein: Identification of precursors and proteolytic products spanning 400 kilodaltons of ORF1a. *Virology* **242,** 288–302.

Schlegel, A., Giddings, T. J., Ladinsky, M. S., and Kirkegaard, K. (1996). Cellular origin and ultrastructure of membranes induced during poliovirus infection. *J. Virol.* **70**(10), 6576–6588.

Shi, S. T., Schiller, J. J., Kanjanahaluethai, A., Baker, S. C., Oh, J. W., and Lai, M. M. (1999). Colocalization and membrane association of murine hepatitis virus gene 1 products and de novo-synthesized viral RNA in infected cells. *J. Virol.* **73**(7), 5957–5969.

Sims, A. C., Ostermann, J., and Denison, M. R. (2000). Mouse hepatitis virus replicase proteins associate with two distinct populations of intracellular membranes. *J. Virol.* **74,** 5647–5654.

Thyberg, J., and Moskalewski, S. (1999). Role of microtubules in the organization of the Golgi complex. *Exp. Cell Res.* **246,** 263–279.

van der Meer, Y., Snijder, E. J., Dobbe, J. C., Schleich, S., Denison, M. R., Spaan, W. J., and Locker, J. K. (1999). Localization of mouse hepatitis virus nonstructural proteins and RNA synthesis indicates a role for late endosomes in viral replication. *J. Virol.* **73**(9), 7641–7657.

Westaway, E. G., Mackenzie, J. M., Kenney, M. T., Jones, M. K., and Khromykh, A. A. (1997). Ultrastructure of Kunjin virus-infected cells: Colocalization of NS1 and NS3 with double-stranded RNA, and of NS2B with NS3, in virus-induced membrane structures. *J. Virol.* **71**(9), 6650–6661.

White, J., Johannes, L., Mallard, F., Girod, A., Grill, S., Reinsch, S., Keller, P., Tzschaschel, B., Echard, A., Goud, B., and Stelzer, E. H. (1999). Rab6 coordinates a novel Golgi to ER retrograde transport pathway in live cells [Published erratum appears in *J. Cell Biol.* 2000, **148**(1)]. *J. Cell Biol.* **147**(4), 743–760.

Ziebuhr, J., and Siddell, S. G. (1999). Processing of the human coronavirus 229E replicase polyproteins by the virus-encoded 3C-like proteinase: Identification of proteolytic products and cleavage sites common to pp1a and pp1ab. *J. Virol.* **73,** 177–185.